



## OPEN ACCESS

## EDITED BY

Abdelmageed A. Elmustafa,  
Old Dominion University, United States

## REVIEWED BY

Chitaranjan Pany,  
Vikram Sarabhai Space Centre, India  
Harry Bikas,  
University of Patras, Greece

## \*CORRESPONDENCE

Sachin Manohar Shinde,  
✉ sachin.shinde@dmce.ac.in

RECEIVED 10 April 2025

REVISED 02 December 2025

ACCEPTED 23 December 2025

PUBLISHED 12 January 2026

## CITATION

Shinde SM, Solanke S, Diwan M, Bhole KS, Salunkhe S, Cep R and Nasr EA (2026) Design and development of a flexural spindle mechanism enabled in micro drilling machine tool within a PLM environment. *Front. Mech. Eng.* 11:1609543. doi: 10.3389/fmech.2025.1609543

## COPYRIGHT

© 2026 Shinde, Solanke, Diwan, Bhole, Salunkhe, Cep and Nasr. This is an open-access article distributed under the terms of the [Creative Commons Attribution License \(CC BY\)](#). The use, distribution or reproduction in other forums is permitted, provided the original author(s) and the copyright owner(s) are credited and that the original publication in this journal is cited, in accordance with accepted academic practice. No use, distribution or reproduction is permitted which does not comply with these terms.

# Design and development of a flexural spindle mechanism enabled in micro drilling machine tool within a PLM environment

Sachin Manohar Shinde <sup>1\*</sup>, Sachin Solanke <sup>2</sup>,  
Mohit Diwan <sup>3</sup>, Kiran S. Bhole <sup>4</sup>, Sachin Salunkhe <sup>5,6</sup>,  
Robert Cep <sup>7</sup> and Emad Abouel Nasr <sup>8</sup>

<sup>1</sup>Department of Mechanical Engineering, Datta Meghe College of Engineering, Mumbai, India, <sup>2</sup>General Engineering Department, Institute of Chemical Technology, Mumbai, India, <sup>3</sup>Department of Mechanical Engineering, Ahmedabad Institute of Technology, Ahmedabad, Gujarat, India, <sup>4</sup>Department of Mechanical Engineering, Sardar Patel College of Engineering, Bhavan's Campus, Bhavans College Rd, Mumbai, India, <sup>5</sup>Department of Biosciences, Saveetha School of Engineering, Saveetha Institute of Medical and Technical Sciences, Chennai, India, <sup>6</sup>Department of Mechanical Engineering, Gazi University Faculty of Engineering, Ankara, Türkiye, <sup>7</sup>Department of Machining, Assembly and Engineering Metrology, Faculty of Mechanical Engineering, VSB-Technical University of Ostrava, Ostrava, Czechia, <sup>8</sup>Department of Industrial Engineering, College of Engineering, King Saud University, Riyadh, Saudi Arabia

The advent of designing flexural systems was to provide accurate micro and nano displacement between the assembly members of the mechanism. Applications that used these mechanisms included linear compressors, optomechanical devices, Stirling engines, cryocoolers, microcheck valves, Flexure-based Electromagnetic Linear actuators, and so on. This paper focuses on the machine-tool fabrication of a novel flexural mechanism encased within the spindle head of the microdrilling head. The mechanism cushioned the micro drill and protected it from permanent damage when encountering undeclared resistance in the material matrix. Furthermore, this paper focuses solely on building a 3-axis drilling machine tool in a Product Lifecycle Management environment. The study follows a systematized approach for validating the machine tool design, starting with the hierarchical assembly of components using various kinematic chains. The next phase involves assigning the necessary motions to these components. The final stage utilizes a virtual controller and post-processor to simulate and control machine tool movements. Validation is then performed on the simulated workpiece to ensure design accuracy and functionality. The key findings of the studies indicate that the designed mechanism can move in and out and can also puncture micro-holes in metal. This is the mechanism's capability, which is the novelty.

## KEYWORDS

flexural mechanism, product lifecycle management, standard simulation, synthesizing, virtual machine tool

## 1 Introduction

The microdrilling process is very challenging because it depends on many factors, including the material being drilled, drill diameter, feed and speed, depth of cut, and coolant used. Further apart from the Ameticon head's ability, the spindle head, along with the in-line of the Z-axis, is significant. Further, the resistance force exerted by the test piece

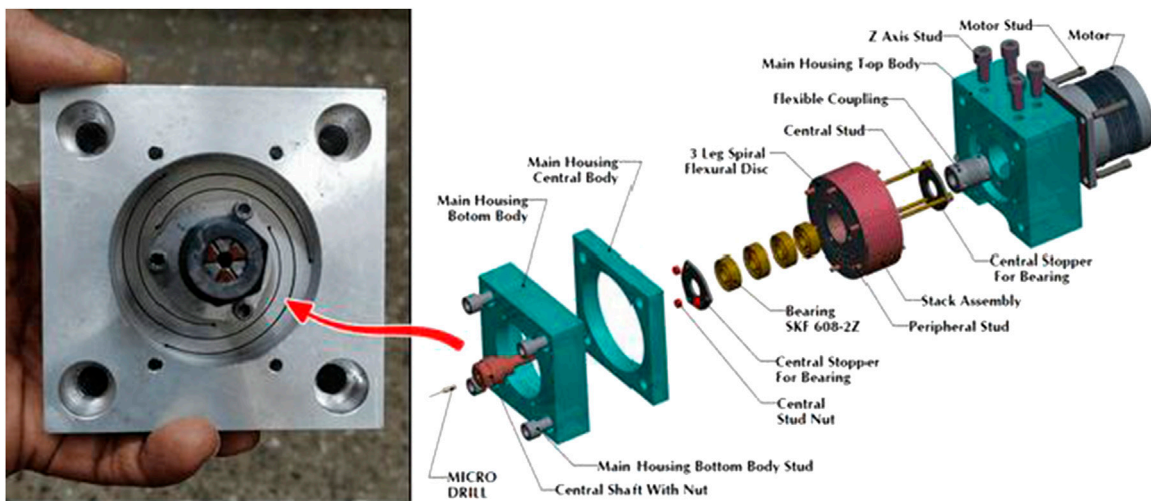


FIGURE 1  
Assembly component of flexural head.

material due to its inhomogeneity may cause additional stress at the micro drill's weakest section. Because micro drills have small diameters, any additional resistance may permanently rupture them. Hence, to address this problem, a flexural mechanism is designed to ensure damping or provide a cushioning effect for the micro drill. This paper focuses on synthesizing a “flexural spindle micro drilling machine tool” within the PLM environment, specifically using Siemens NX 12. The flexural spindle head, which encases the flexural mechanism, tends to move into and out of the direction about the axis of the flexural mechanism. The complete mechanism is clamped to the periphery of the casing and opens on one side (toward the bed side). The bearings arrest the spindle within the flexural mechanism. The spindle now turns out to be a cantilever in design and construction. The spindle moves in and out of the fro direction. The spindle uses a collet chuck to clamp the micro drill. In micro-hole drilling, when the drilling thrust is inside the material, the resistance force provided by the workpiece specimen is greater than the resistive force on the minimum cross-section of the micro-drill—the micro-drill breaks. A flexural mechanism between the drill and the spindle body overcomes this problem. The mechanism provides micro-displacement and cushioning to the micro-drill, preventing permanent breakage. This is the new novelty established in the paper, which contrasts with the conventional micro-drilling process on CNC machines. The basic design of flexural mechanisms mainly showed interest for the dynamic balancing of the compressor shaft used in cryogenics. As this was used in a spacecraft, it was difficult to oil. The authors have tried to use this bearing as a “micro positioner” in dynamic conditions. This is a contribution to society. Further, for the drilling process, the authors have performed a drilling simulation and confirmed an error-free tool path. The tool paths obtained are collision- and gouge-free, as shown in a visual simulation of the tool, and the machine tool components are visible. Checking the tool path in the vicinity of the machine tool is only available in the PLM environment. The PLM environment provides a perfect virtual environment where, as with the rest of the CAM packages, error-free paths are available. The integration of

Product Lifecycle Management (PLM) platforms with manufacturing tools such as CAD, CAE, and CAM has become increasingly prevalent, as [Sanchez Gomez et al. \(2017\)](#) highlights. This integration provides a comprehensive product development environment, facilitating a seamless transition from product conception through its entire lifecycle. The PLM environment offers significant advantages, including reduced operational costs and the establishment of a concurrent engineering framework. In this integrated setup, CAD tools enable behavioral and synchronous modeling, CAE tools refine design optimization, and CAM tools handle detailed manufacturing and toolpath generation. Guerra-Zubiaga has emphasized the necessity of advanced methods and digital tools in a cross-functional business environment, asserting that PLM platforms enhance knowledge transfer and information flow throughout the product lifecycle ([Sanchez Gomez et al., 2017](#)). Chan further discusses the role of graphical solutions in integrating product and process design, noting the competitive advantage of virtual manufacturing. This virtual environment allows for high-quality product development at reduced costs and faster timelines. Despite the availability of various CAD/CAM/CAE software packages, Chan also highlights limitations in data exchange capabilities, underscoring the need for an “Integrated Product and Process Design (IPPD) approach ([Chan, 2003](#)). The principles of interactive design and manufacturing, as described by Fischer and Coutellier, support lateral information sharing and innovation through virtual testing, reducing the time and cost associated with physical manufacturing ([Fischer et al., 2006](#)). Using graphical simulations, as Abdul Kadir and Kumar explored, helps avoid miscalculations, accelerates time-to-market, and minimizes waste ([Kadir et al., 2011](#)). Recent advancements in virtual machine tool simulation within the PLM framework have enabled detailed simulations of machining operations, including tool path and collision detection ([Altintas et al., 2005](#)). The capability to simulate machine tool movements and process parameters in real time enhances training and operational accuracy. Despite progress, the transition of virtual simulations to industrial applications remains challenging, as noted by [Lagarrigue et al. \(2006\)](#). Hajicek

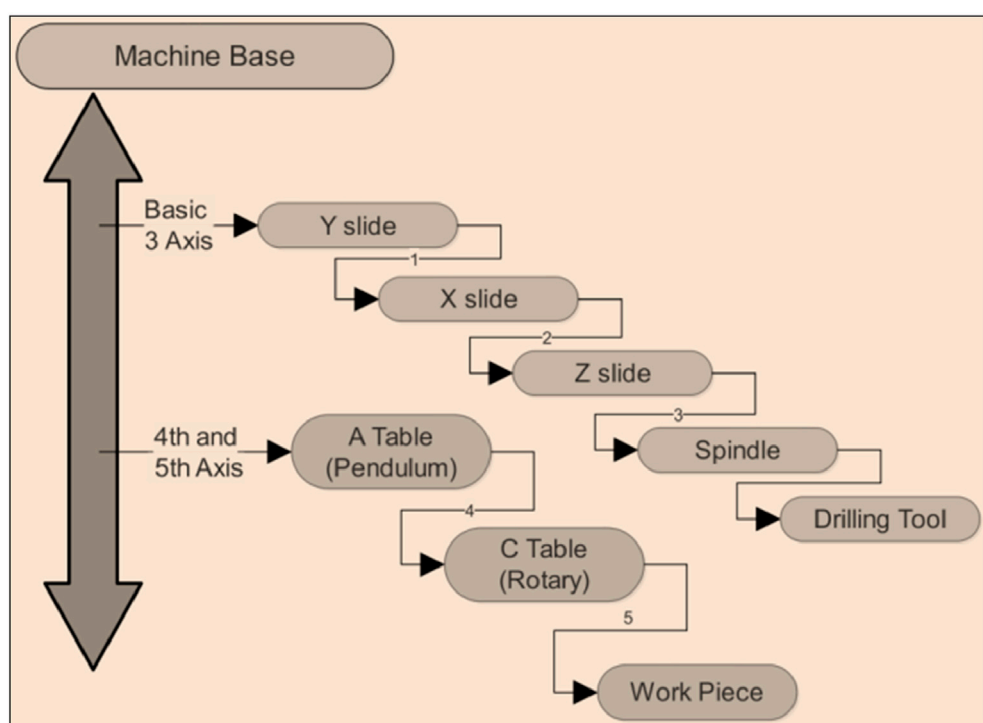


Table -Table

Head Head

Head Table

a



b

FIGURE 2  
(a) Various five-axis machine tool configurations. (b) Hierarchical components of the five-axis kinematic chain in a table-table configuration.

discusses the creation of a machine tool simulator using an optimized layout and a Common Simulation Engine (CSE) template, incorporating the machine tool kinematic structure, post-processor, machine coordinate system (MCS) driver, and a service library. [Lisboa Borsatti et al. \(2014\)](#) defines a virtual environment as an advanced user interface that facilitates real-time interaction and visualization ([Lagarrigue et al., 2006](#)). Ercetinet al. provide a comprehensive overview of the evolving role of image processing in machined surface analysis, emphasizing its growing importance across multiple industries. Integrating deep learning, artificial intelligence (AI), and machine learning (ML) into image processing algorithms has significantly enhanced surface analysis capabilities ([Ercetin et al., 2024](#)). These

advancements have improved accuracy and efficiency and expanded image processing applications into sectors such as healthcare, manufacturing, aerospace, automotive, and agriculture. In traditional and CNC machining, image processing has become essential for applications such as tool wear analysis, workpiece origin detection, automatic CNC program generation, and tool setting. The ability to conduct real-time inspections and predict surface roughness during machining has dramatically reduced downtime and enhanced product quality. Similarly, image processing techniques have revolutionized surface texturing and quality monitoring in micromachining, enabling more intricate and precise work. Additive manufacturing has also benefited significantly from advances in image processing. These

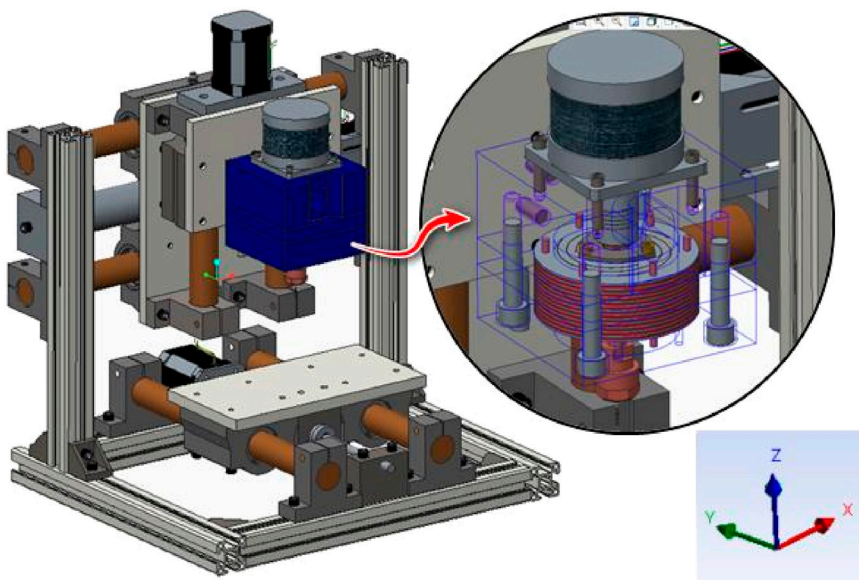


**FIGURE 3**  
Axis orientations of the three-axis flexural spindle head micro drilling machine.



**FIGURE 4**  
Assembly component of flexural head.

advancements have facilitated in-process defect detection, real-time monitoring, and quality enhancement during pre- and post-processing operations. As a result, overall efficiency and quality control in additive manufacturing have improved considerably. The paper explores prospects and potential developments in image processing. The emergence of high-resolution and 3D imaging, coupled with AI and ML advancements, is expected to further enhance quality control, predictive maintenance, and productivity across industries. However, challenges such as data privacy concerns and the demand for skilled professionals to manage these technologies remain key considerations. In conclusion, this review highlights the transformative impact of image processing in machined surface analysis. Its integration into machining processes has streamlined quality control, increased efficiency, and paved the way for further innovation and research. As

technology continues to evolve, the potential applications of image processing in industrial and scientific fields will continue to expand, ushering in a new era of precision, efficiency, and data-driven decision-making. Further, Pimenov et al. comprehensively review image processing applications in machined surface analysis, focusing on tool condition monitoring (TCM). It highlights the integration of artificial intelligence (AI), machine learning (ML), and deep learning to enhance accuracy and efficiency across the manufacturing, aerospace, and healthcare industries (Pimenov et al., 2024). Both direct and indirect image-processing methods for tool wear analysis are explored, with direct methods enabling real-time measurement *via* synchronized cameras, while indirect methods estimate wear based on factors such as chip geometry and surface roughness. Advanced techniques such as neural networks, image thresholding, and tool shape descriptors improve tool wear recognition and classification. Image processing is also crucial in additive manufacturing for defect detection and quality control. Future advancements in AI, IoT, smart manufacturing, and digital twins will further revolutionize machining processes, improving predictive maintenance and productivity. The paper concludes that image processing is a transformative tool for quality control and efficiency, shaping the future of industrial automation and precision manufacturing (Pany and Rao, 2004; Pany, 2023). As shown in Figure 1. Section 2 explains the concept of the flexural design head; Section 3 outlines the methodical procedure for machine tool construction; Section 4 details the kinematic chain assembly; Section 5 addresses coordinate system assignment; Section 6 explains the virtual controller; and Section 7 discusses the machine tool's validation. This study represents preliminary work on machine tool design, with physical movement analysis outside its scope.

The flexural bearing in the flexural cartridge functions as a linear guide, moving back and forth to alleviate the axial load applied to the drilling workpiece (Shinde et al., 2022; Shinde and Lekurwale, 2018).

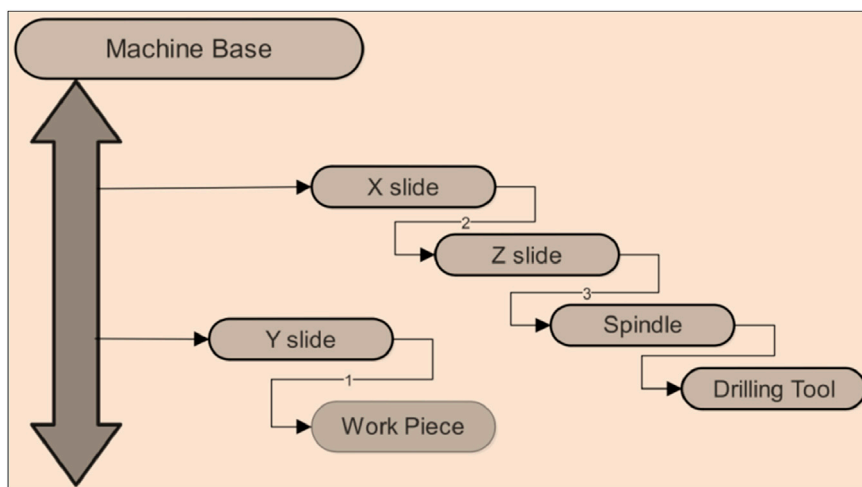


**FIGURE 5**  
Three-axis flexural spindle head showing kinematic chain component hierarchies.

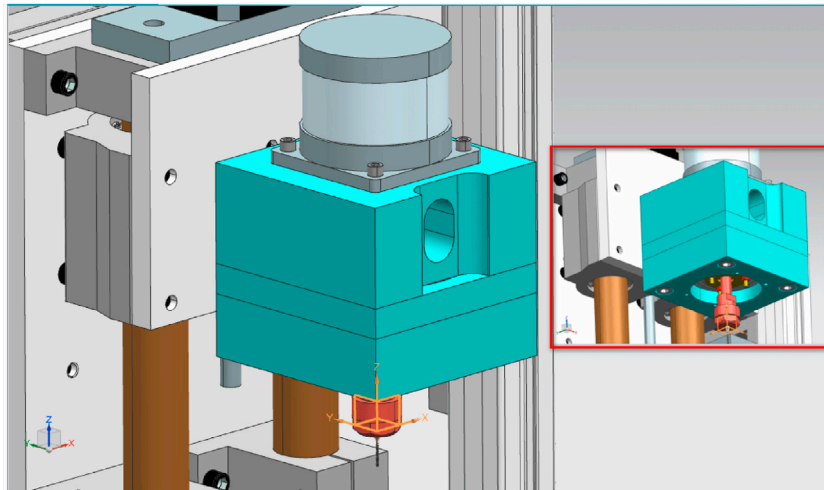


**FIGURE 6**  
Machine zero junction at maximum Z limit, showing the upward direction.

The movement of the flexural element carrying the shaft loaded in the bearing adjusts itself to the resistance encountered (Shinde and Lekurwale, 2019). Some researchers have employed external media to achieve precise linear movement (Bhole and Janbandhu, 2018; Bhole et al., 2019). This mechanism effectively reduces the force exerted on the micro drill, thereby preventing permanent damage (Gandhi et al., 2013; Gandhi and Bhole, 2013) or fracture (Shinde and Lekurwale, 2022; Shinde and Lekurwale, 2021; Shinde et al., 2023). Before this concept, Bhole and Janbandhu designed single-pole machines capable of thrilling in acrylic (Bhole and Sonavane, 2018). When this machine was tested for metal drilling, the Z-axis deflection was too high, rendering drilling impossible. Further in the paper, a double-column frame construction was erected for greater strength, with a reduced flexural diameter and a greater number of discs in the assembly.

## 2 Methodology

For the development of machine tools done on PLM. The detailed procedure of PLM is as follows. The first step involves detailed geometric modeling of individual parts and assemblies, ensuring proper constraints are applied. Essential information required alongside the design includes the table work surface area, the travel distances of each axis, the work envelope, the total usable distance from the bottom of the spindle chuck to the tabletop, the vertical distance between the bottom surface of the main housing and the chuck, and tool storage capacity. All this information is stored in a single folder to facilitate linking to the respective post-processor and controller files. The main folder, named after the machine tool, contains three subfolders: a graphics folder with all designed 3D models and the assembly

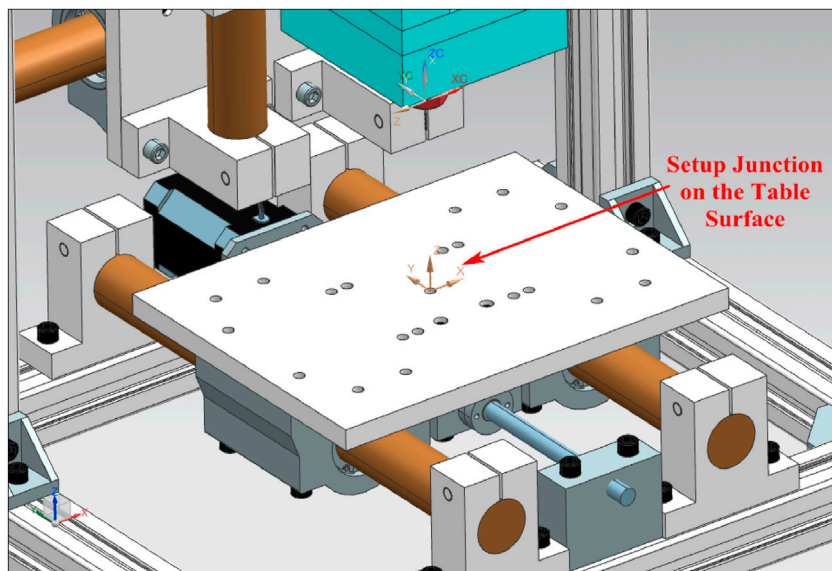


**FIGURE 7**  
Setup junction placed on the table surface and matching the orientation of the machine zero.

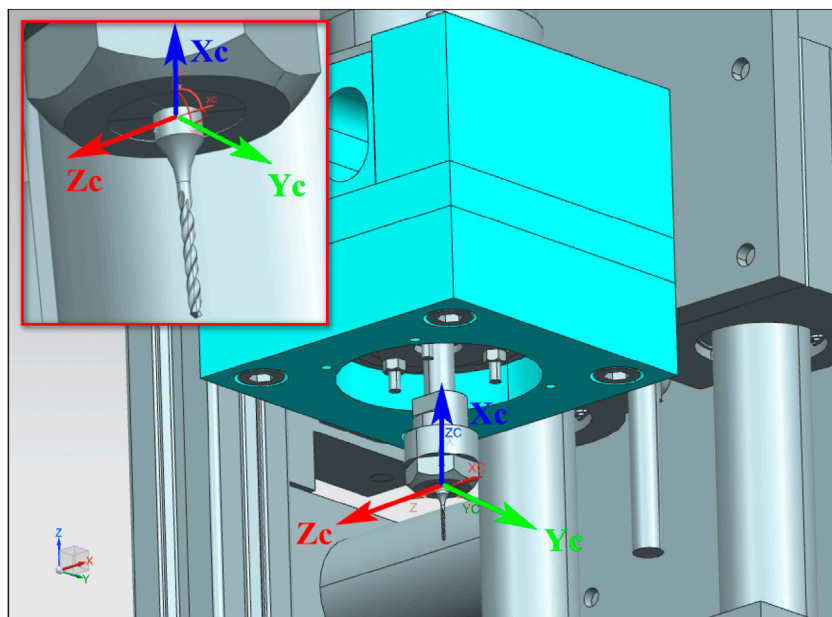


**FIGURE 8**  
Representation of the tool mount junction (vertically upwards) placed on the spindle's axis.

file; a CSE folder with supporting files, including the machine home position and tool change programs; and a postprocessor folder that stores all supporting files for the post-processor. The second step involves using a PLM system to identify the CAD model. It includes assigning junctions and separating workpiece holding from tool holding. All information is recorded in the SIEMENS NX software. The third step involves post-processor assessment of the machine tool. The PLM software allows for modification of the post-processor, and a standard in-built post-processor can be selected

as needed. All integrated data from various post-processors is stored in the machine database file. The complexity of the piece decides the ideal machine tool for machining. 5-axis machine tools can machine all complex workpieces. It has the minimum axes to machine all sides of a workpiece. The kinematic chain representation depends on the machine's structure. The configuration of a five-axis machine can be “table-table, head-head, or head-table (Lin and Koren, 2000; Cao and Li, 2022). The standard configuration of a 5-axis configuration includes three translational axis, i.e., X, Y, and

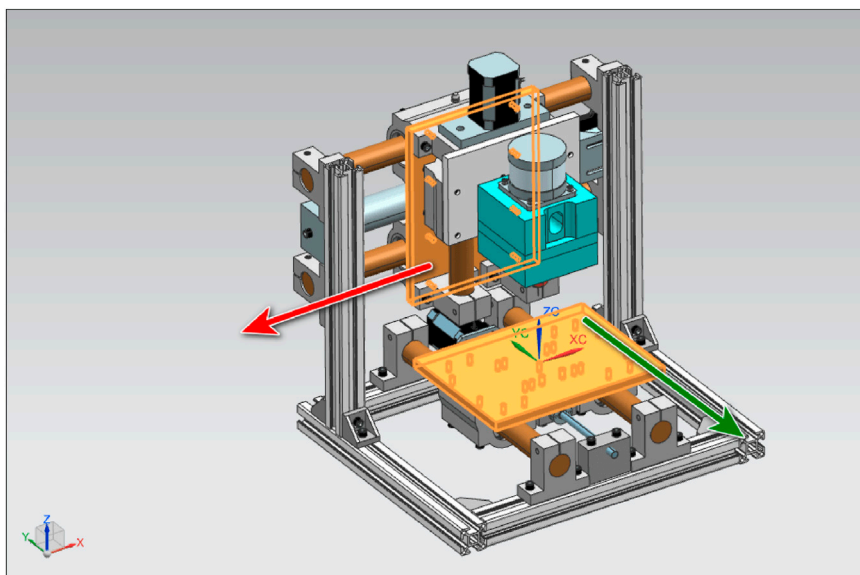


**FIGURE 9**  
X and Y-axis representation for positive motion (X - red arrow: positive Y green arrow).

Machine Tool Navigator - Machine Tool Builder								
Name	Classification	Junctions	Axis Name	Axis Number	Initial Value	NC Axis	Axis Type	Axis Limits
MACHINE_TOOL								
MACHINE_BASE	_MACHINE_BASE	MACHINE_ZERO_JUNCTION*						
Y_SLIDE			Y	1	0	✓	Linear	-72, 106
SETUP	_SETUP_ELEMENT	PART_MOUNT_JCT						
BLANK	_WORKPIECE,_SETUP_ELEMENT							
PART	_PART,_SETUP_ELEMENT							
FIXTURE	_SETUP_ELEMENT							
X_SLIDE			X	2	0	✓	Linear	-74, 58
SPINDLE		S*	Z	3	0	✓	Linear	-76, 4

**FIGURE 10**  
Virtual environment representation of the machine tool.

Z-axis and two rotary axis, i.e., A and C, placed on the bed (Lee and Lin, 2010; Kadir et al., 2011), as shown in Figure 2a (in some cases, it may be the B and C axes) (Yuksel et al., 2020; Wang et al., 2023). The placement of the fourth and fifth axes depends on their integration with the standard axes, where the X-axis, Y-axis, and Z-axis are the parent axes, and A, B, or C are the child axes. Figure 2b represents the “table-table” Configuration, head-table, or head-head.” (Choi et al., 2015; Wang et al., 2022).

Figure 2b illustrates the five-axis kinematic chain component hierarchy of a table-table configuration (Bohez, 2002). The “kinematic chain” is a geometric representation of the assembly components that depicts the parent-child relationships. The body frame serves as the parent for the remaining assembly components, providing the machine’s zero-coordinate reference system. Similarly, the cutting tool, its fixture, and the workpiece also form part of the kinematic chain. Therefore, the components of the machine tool are classified according to the parent-child

relationships defined during the machine-building process. A kinematic chain is specifically applied to the machine tool assembly model (Wang and Yu, 2006). The parent-child relationship is maintained between the assembly members. The frame of the machine tool becomes the parent of all. The X-slide movement is done on the frame, making it the frame’s child. Refer to Figure 3, which shows the same. In this manner, the kinematic chain is established. Further, upon successfully assigning the kinematic chain, a green check mark appears (see Figure 9, which shows the fully defined assembly model in the PLM environment). Figure 9 shows the NC axis number defined in Figure 4, along with the parent-child relationship.

Figure 3 exhibits the geometric model of the micro drilling machine tool, while Figure 4 displays the manufactured spindle head for the micro drilling machine tool. These figures show that two essential components are the work-holding components (the table) and the tool-holding components. The machine tool is divided into

```

File Edit Format View Help
(#19696-0 : rotating table coordinate system for G43.4/5. Change in INI program to 32 for non-rotating workpiece coordinate system)
#19696-32
(This part sets the position of the reference point G28)
G54
(Implement the setting of the reference point unit dependent)
G10L52
N1240P1R178
N1240P2R132
N1240P3R000
G11

```

FIGURE 11  
Machine home position for FANUC controller.

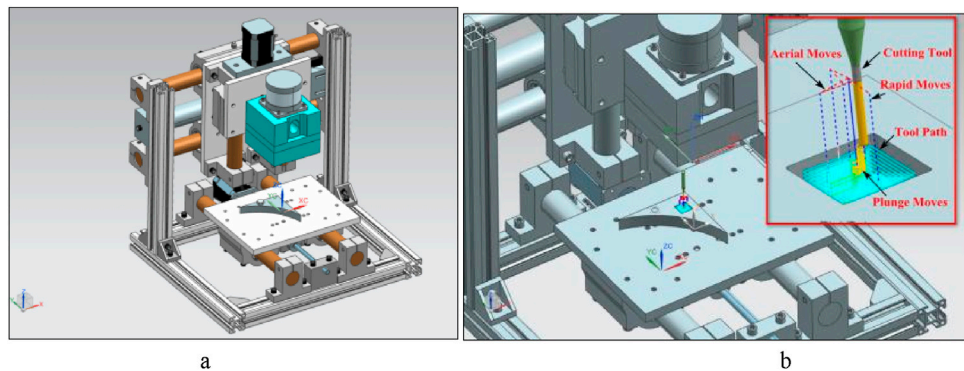


FIGURE 12  
(a) Milling Setup in a virtual environment (b) Tool-path programming in a virtual environment.

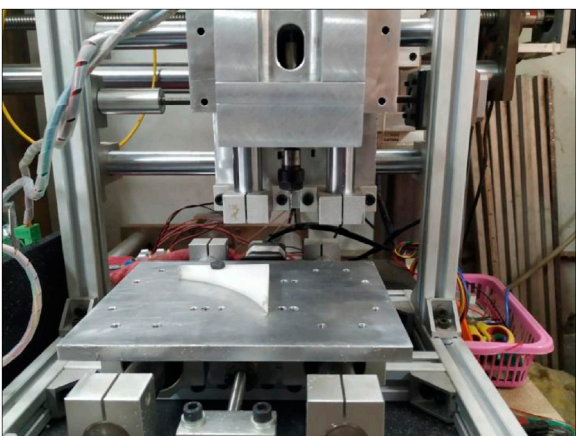


FIGURE 13  
Workpiece on the designed machine tool.

tool-holding and work-piece-holding components. The parent-child hierarchy aids in constructing the virtual machine tool. Figure 5 illustrates the basic kinematic chain of the three-axis flexural spindle micro-drilling machine tool. The PLM platform in SIEMENS NX software (Siemens Product Lifecycle Management Software, 2013) facilitates the construction of a virtual machine tool based on the defined kinematic chain (Shinde and Lekurwale).



FIGURE 14  
Validation of programs driven by a virtual environment (milling).

After constructing the kinematic chain, the next step is to assign the junction coordinate system for the designed machine tool. This step establishes and develops parent-child relationships among the various components of the machine tool assembly. The junction coordinate system, along with the axis vector, stores the direction, operating limits (travel), type of motion (linear or rotary), and the nature of the motion (e.g., whether the axis is NC or not) when the information is supplied to the PLM platform. Establishing junctions, similar to constructing the kinematic chain, is crucial. Without junctions, each part would be isolated, with no relationships to other parts. For example, the Y-axis is assembled on the body structure

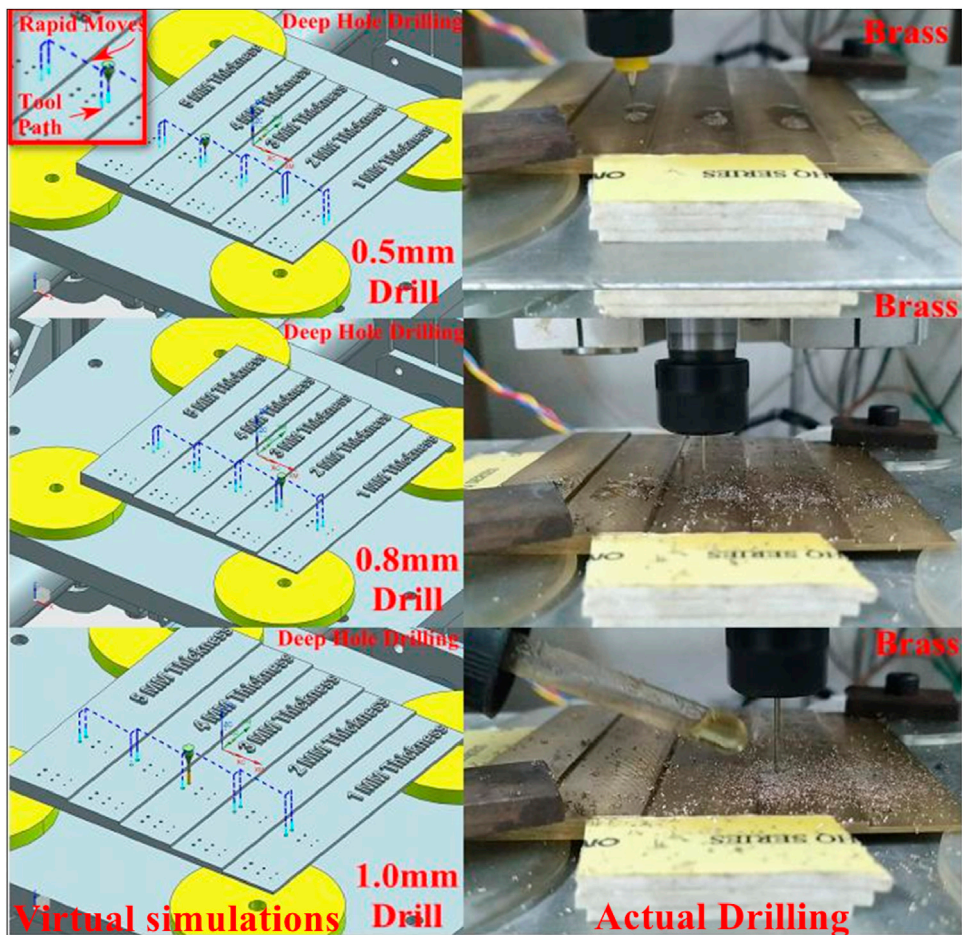


**FIGURE 15**  
Validation of programs driven by a virtual environment (drilling).

parallel to the base, while the X-axis is assembled on vertical poles clamped to the base body structure. The X and Y-axes are independent and are considered children of the base body, which acts as the machine's parent junction. The machine's imaginary zero is a coordinate system floating within the operating limits of all axes. In this design, the machine zero is perfectly aligned with the spindle axis at its uppermost limit. The Z max limit falls within the bounds of both the X and Y-axes.

Each component assembled in the machine tool has a unique junction coordinate system inherited from the machine's zero junction. This inheritance enforces the parent-child relationship within the kinematic chain. The specified junctions are "setup junction and tool mount junction." A setup junction identifies a specific workpiece or fixture point for clamping purposes. Similarly, the tool mount junction specifies the tool's mounting position, typically defined by the spindle's concentric surface. Additionally, if there is a rotary component in the system, it will be specified by a junction created on the rotational axis of the element. Figure 6 shows the machine's zero junction, while Figures 7, 8 illustrate the setup and tool mount junctions, respectively.

The movement of the tool about the clamped workpiece defines the machine axis. In the designed machine tool, the Z-axis moves in the positive direction, while the Y-axis slide moves in the negative

direction. When a rotary table is used, the direction of rotation follows the right-hand rule. For example, the machine table will rotate counterclockwise if the spindle rotates about a positive axis (X, Y, or Z). The asymmetric layout of the machine's axis drives allows effective utilization on either side of the machine, with zero, which is located at the table's center and aligned with the spindle axis. The vertical distance between the lowest position of the Z slide and the workpiece surface on the table is 45 mm, while the distance at the topmost position of the Z slide is 125 mm. Thus, the Z-axis travel is 80 mm. Figure 9 illustrates the positive directions of the X and Y-axes in red and green, respectively, with the positive Z-axis represented vertically upwards (Siemens Product Lifecycle Management Software, 2013). The PLM platform provides additional information, including classification, junction, axis name, initial value, NC axis, and axis limits, as depicted in Figure 10. The setup element shown in Figure 10 is the default template; as we have not used it, it does not apply to the manuscript. Setup elements are used when complex jobs with specialized fixtures are required, as they are not applicable in research studies.

The function of the "post-processor" applied to software-driven tool paths is to convert the NCL file into G and M codes, which are purely numerical values. The virtual controller interprets these NC codes in the PLM platform and generates equivalent signals supplied

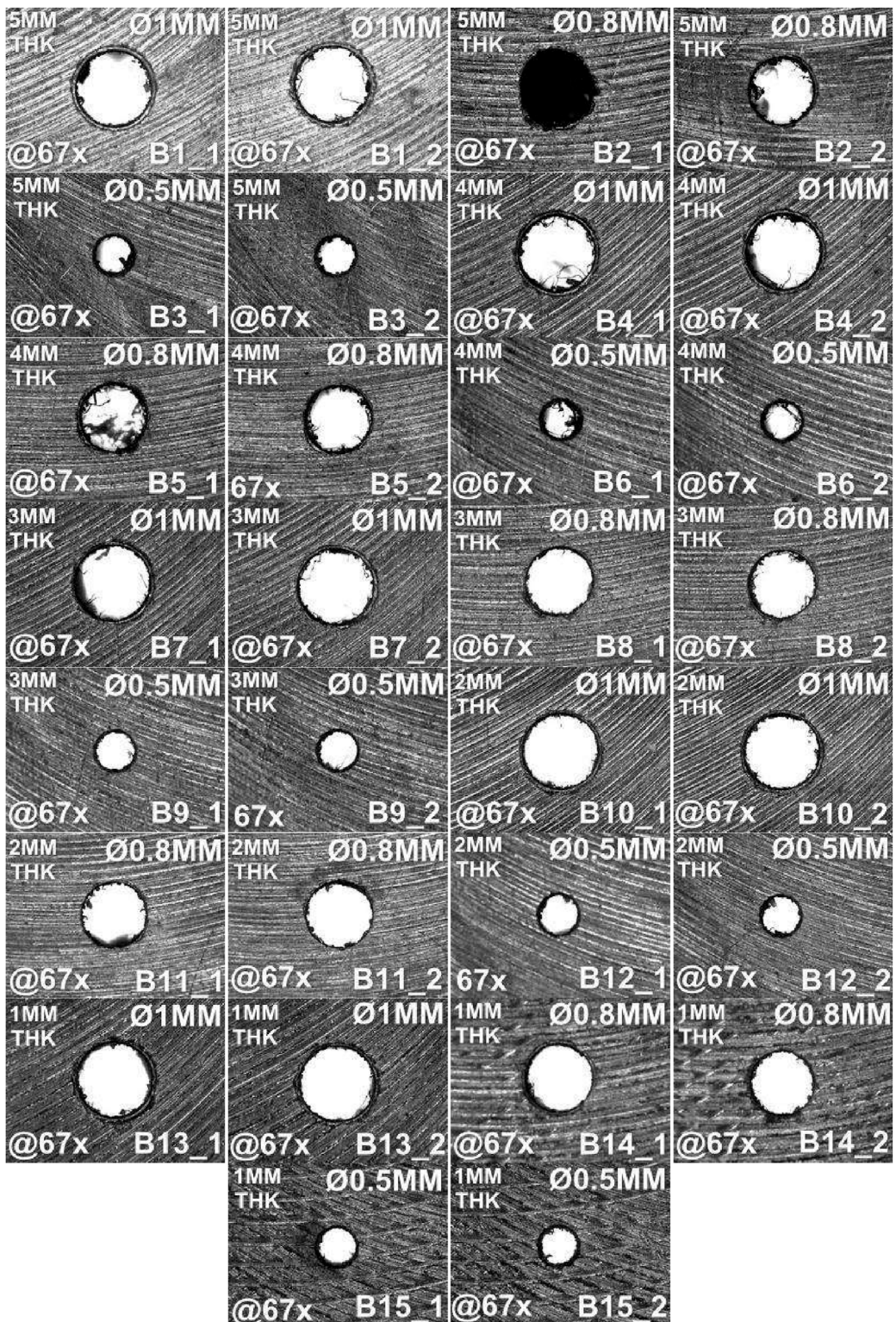


**FIGURE 16**  
Rapid-I images of holes drilled by CNC machine in brass specimens.

to various machine tool components. To function efficiently in the virtual mode, the virtual machine tool (VMC) extracts all relevant information, such as axis names, axis operating limits, part mounting locations, tool mounting locations, and tool mounting

orientations (Lin, 2013). The post-builder simulates machine operations in the virtual environment. The SIEMENS NX post-processor builder requires information from the GUI interface. This data includes operating units, home position, machine travel limits,

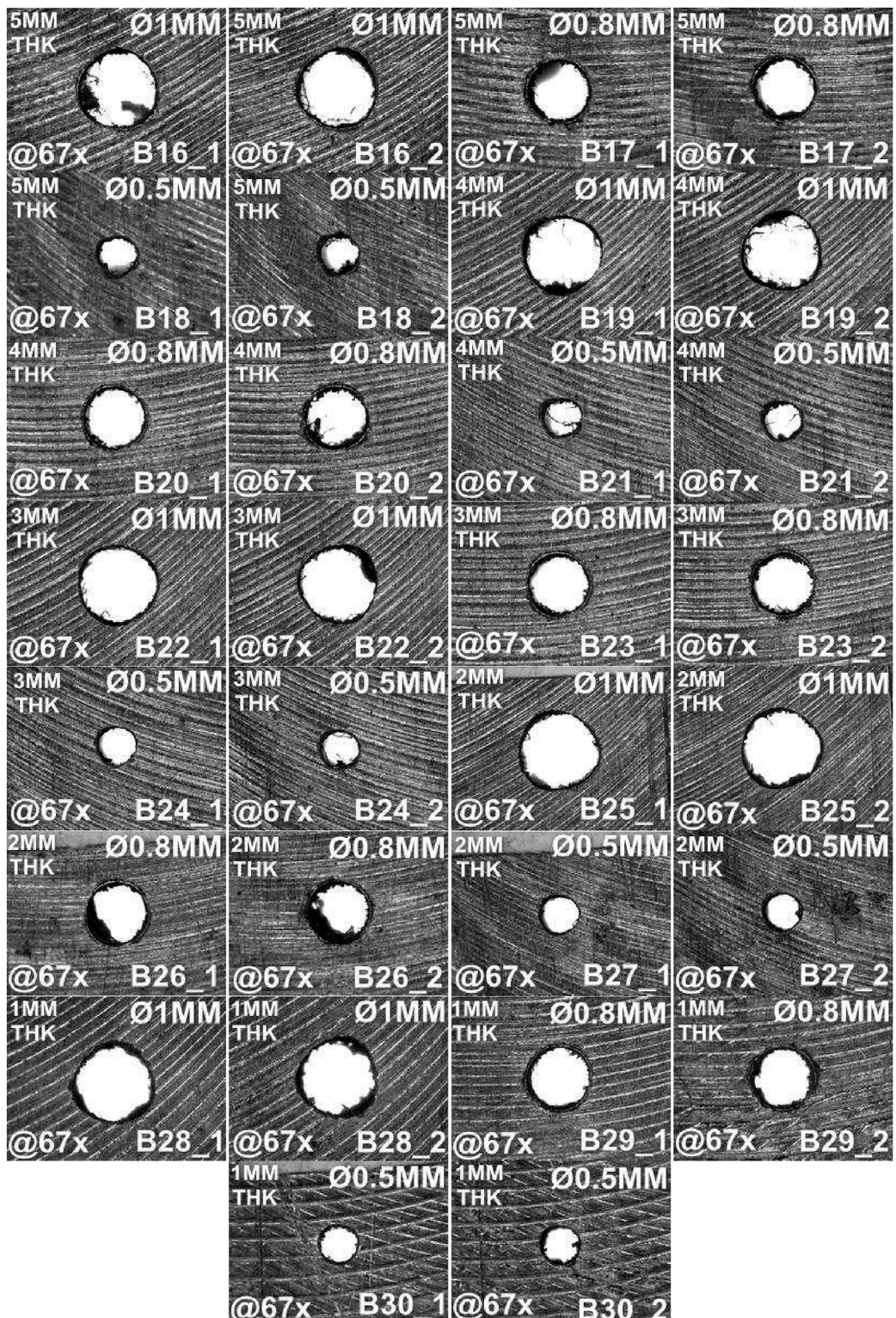


**FIGURE 17**  
Rapid-I images of holes drilled by flexural spindle in brass specimens.

resolution of each step, number of axes, traverse feed rate, and motion resolution. The virtual controller needs a starting point to execute tool motions, which are generally based on the machine's zero reference point. Typically, the G28 command sets this reference

point, moving all slides to the set reference position, which is generally maintained at the maximum Z-axis travel height. In SIEMENS Nx12, the m/c reference position can be set using the.inc. file, an initialization file starting with block N1240.

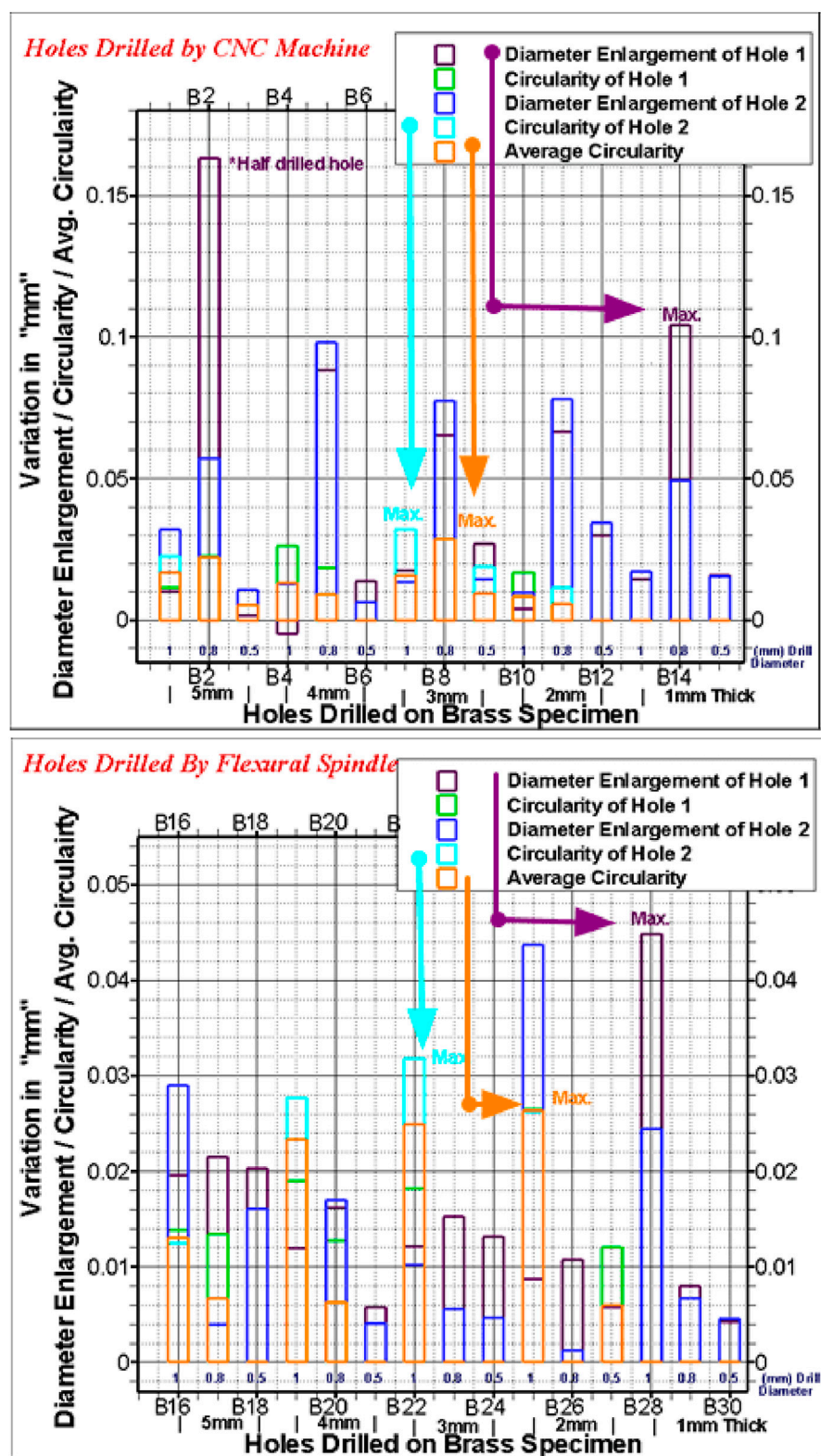


FIGURE 18  
Assessment hole drilled by CNC and designed spindle head.

Figure 11 shows the last three digits in every line, indicating the predefined X, Y, and Z limits. In the designed machine tool, there is no provision for an extra tool mount; the tool in the

spindle is the only one programmed for use. The tool program (.prg file) executes the tool change concerning the initial reference point.

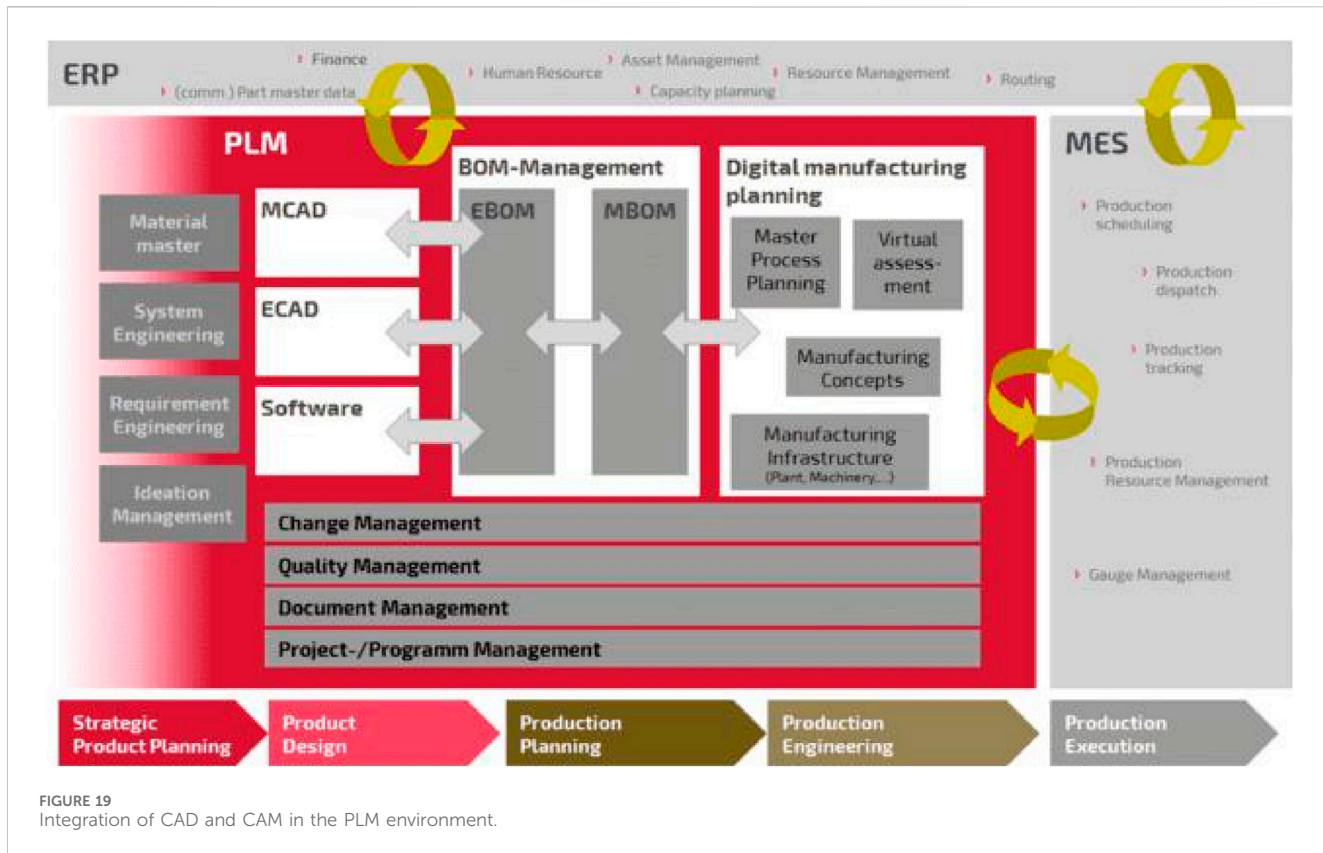


FIGURE 19  
Integration of CAD and CAM in the PLM environment.

### 3 Validation of the proposed model

The virtual machine tool requires specific information about the workpiece placement and clamping fixtures. It also needs machining strategies based on material strength. To effectively utilize the setup, a systematic procedure is employed. In the CAM environment, the modeled workpiece and clamping fixtures are assembled and then transferred to the virtual machine tool (Figure 12a). The setup requires systematically selecting the coordinate system and metal-cutting strategies, along with appropriate tooling. The tooling requires appropriate operating speed and feed rates based on the cutter's out-stick and diameter. The workpiece is clamped on the fixture, which was designed earlier. Local programming is performed around the job surface. After preparing the programs, the software allows the retrieval of the machine designed earlier in the CAM module. When the machine is called, the setup junction associated with the workpiece and fixture is matched with the assembly at the table surface. Collisions can be checked during programming or during simulation of the workpiece, as shown in Figure 12b. The final segment involves simulating the workpiece in real-time. The simulation process's strength lies in its ability to model interactions among machine components, the workpiece, and the fixture. This means the predefined parent-child relationship in the software will run the summation process on the screen and display real-time updates. All the designed work envelopes (outer sizes of the assembly components) will be used in simulations and calculations. The software detects collisions between the workpiece and m/c components, or between the workpiece and

the tool, and indicates any collision limits. Additionally, the software detects any axis overtravel beyond specified limits. Figure 13 shows the actual setup before the machining of the pocket.

The machine tool is validated by machining a square and circular pocket on the workpiece. The job was directly clamped to the table surface while machining was performed within the material. The first trial was conducted on Delrin material due to its softness, using a one mm-diameter tool. After completing the simulation without errors, the program was transferred to the machine tool for actual cutting. A detailed examination confirmed that all slide moves, including the rapid feed moves, were as desired. Figure 14 shows the cutting process in progress. Similarly, Figure 15 shows the drilling programs created in the virtual environment and the final drilled work specimen. This test was performed on a brass specimen. The drilling speed is 12,000 rpm at 1 mm/min in a peck drilling cycle with kerosene coolant.

Virtual simulations help understand the actual motion of the tool slides that carry the spindle head. The actual tool path generated is loaded into the simulator using a numerical cutter location file. The simulator reads the coordinate cutter movement points. The movement of the slides is shown on the screen with a fixed base. All the slides work in tandem, and the cumulative moment is displayed on the screen. This is the advantage of the used method. Further, the micro-drilled holes in the brass specimens by the flexural spindle head were compared with those drilled by a regular CNC machine. Figure 16 shows the images of holes drilled by the CNC machine under the Rapid I machine tool. Each drill creates two holes in CNC drilling, with the designed spindle head. B1\_1 and B1\_2 are the two

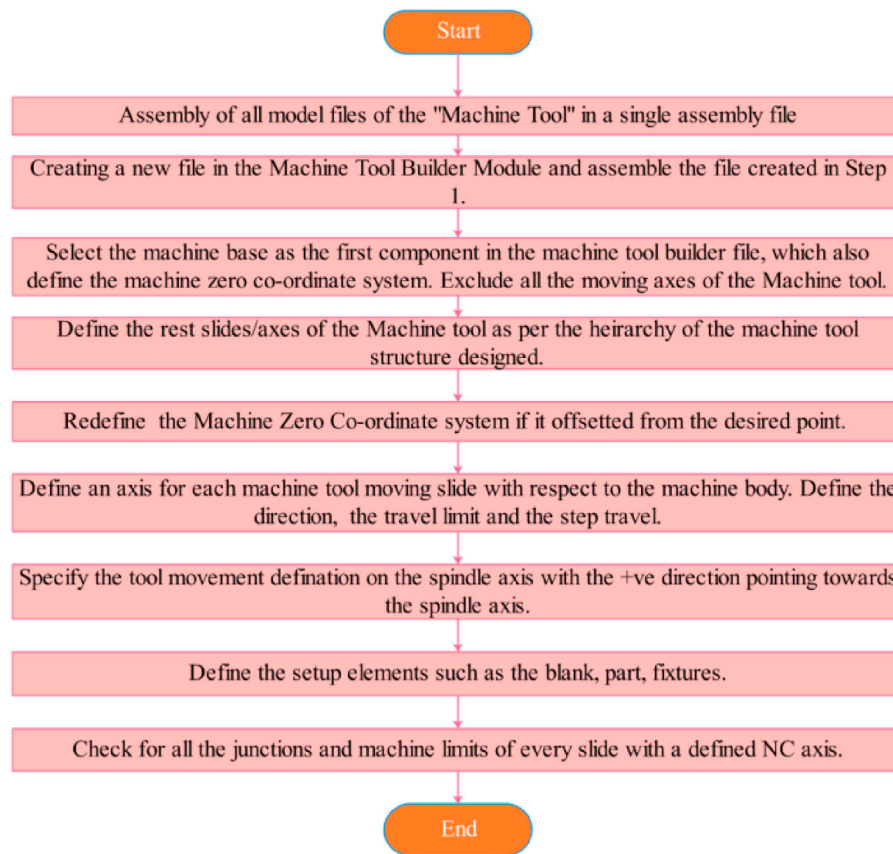


FIGURE 20  
Flow chart representing kinematic modeling in Siemens' software.

holes drilled on the 5 mm thickness step by CNC drilling. Further, B2\_1 and B2\_2 are drilled with a 0.8 mm drill on a 5 mm step, and similarly, B3\_1 and B3\_2 are drilled with a 0.5 mm drill on a 5 mm step. Further, the same process was carried out for 15\_1 and 15\_2 with a 1 mm thickness step. The brass specimen shown in Figure 15 features steps from 1 mm to 5 mm thick. Drills of Ø0.5 mm, Ø0.8 mm, and Ø1 mm were used for drilling operations. Holes numbered 1 to 15 were made using CNC drilling, while holes numbered 16 to 30 were drilled by the designed spindle head. Refer Figure 17. Every step has two holes drilled adjacent to each other. The diameter enlargement and the circularity of the holes drilled were analyzed under the CAD environment of the Rapid machine tool. Figure 18 shows the actual difference between the desired and drilled values for diameter enlargement and circularity at positions 1 and 2.

Furthermore, for the Flexural spindle head, drilled holes in the brass (specimen), the maximum diameter enlargement was 0.0448 mm (44.8  $\mu$ m) at position "B28\_1". The "maximum average circularity" achieved was 26.4  $\mu$ m at positions B25\_1 and two others. Similarly, for the holes drilled by CNC, the maximum diameter enlargement was 104.3  $\mu$ m at position "B14\_1," and the maximum average circularity was 28.6  $\mu$ m at positions "B8\_1 and 2". The differences in diameter enlargement and maximum average circularity between the two methods were 59.5  $\mu$ m and 2.2  $\mu$ m, respectively.

## 4 Results and discussion

The integration of CAD and CAM can be easily handled by uploading the required CAD or assembly files in the user login. The main objective of the PLM environment is to maintain the track of the entire department under one roof—the live positions of the manufacturing as a whole. Items are seen in real-time. The advantage of PLM is that changes in design may or may not be incorporated, and the current status can also be tracked, enabling us to determine whether the change is feasible. Furthermore, if the design department releases the R1 version for manufacturing, it is floated in the system for manufacturing. All supporting activities are also triggered, and necessary action is taken. Now, if the CAD department issues any R2 version for some reason. The system automatically displays a pop-up to all shareholders connected to the system. The model is compared because users have the same file and the same platform. Generally, the programmer generates the program using the CAD model. After the program is generated, the developed programs are checked for collisions or gouges with the machine tool or the workpiece. If any programs are found to have crashed, they are modified and regenerated. Hence, collision and gouge checks are built into the CAM module. There is no separate error-checking mechanism for the virtual controller. The results indicate that a virtual machine can be successfully implemented in NX 12 s machine tool builder module and in other parallel PLM

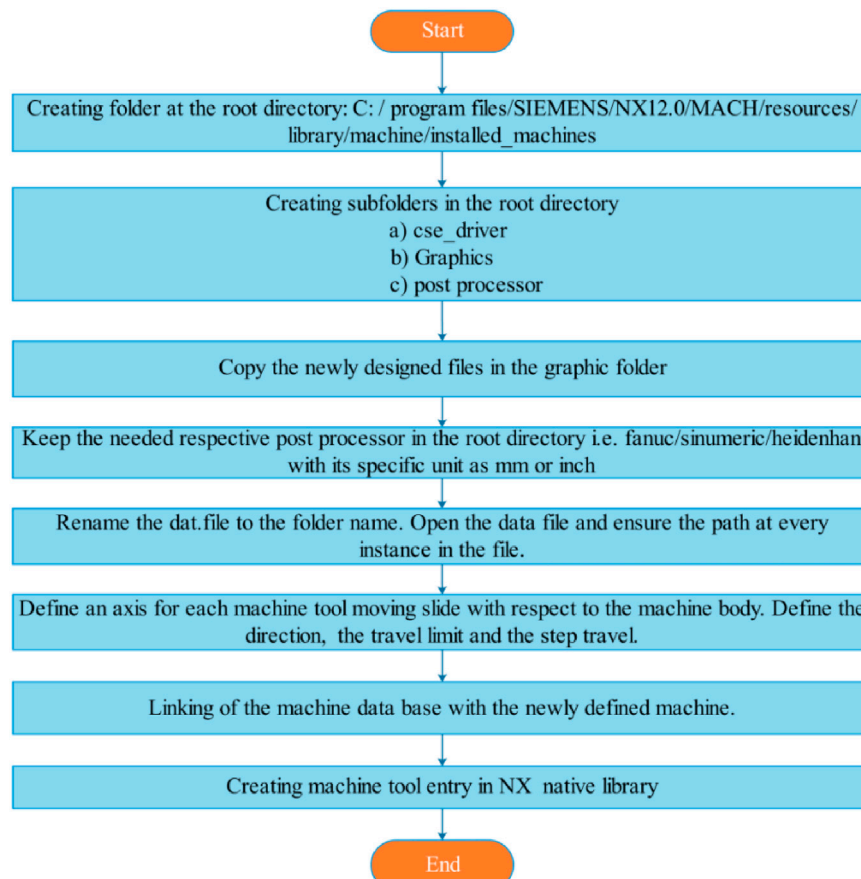


**FIGURE 21**  
Flow chart showing the machine tool in NX's library.

platforms. The virtual environment produces results identical to those obtained with commercial methods, with significant savings in time and money. This demonstrates that it is possible to generate accurate results without a machine tool, provided a PLM platform is available.

Furthermore, results from one PLM platform can be viewed and executed in reality, enhancing the PLM environment's utility in commercial and industrial scenarios. The integration of CAD and CAM is shown in Figure 19. The virtual setup can easily detect axes' overtravel, which would be challenging if the job were done conventionally on the machine. In a physical setup, overtravel triggers alarms and results in lost production time due to job reference shifts from slide collisions. This issue is easily detected and rectified in a virtual environment, allowing for adjustments to the tool path to prevent collisions.

Additionally, depending on the job's complexity, the exact fixture design can be finalized by simulating intricate simultaneous movements of the tool axes. This helps determine the minimum fixture thickness required for the tool axis to move collision-free. The minimum L/D ratio (tool out-stick/diameter) for optimal cutting characteristics and finish can also be defined. The exact remaining stock on the job can be identified by extracting the final stock model left on the workpiece. (Puig et al., 2003). Finally, the general procedure for designing a machine tool with any number

of axes can be summarized using the flowcharts shown in Figures 20, 21. These figures illustrate the creation of the kinematic model in SIEMENS NX 12 and the creation of a machine tool entry in the NX native library, respectively. Further, if any researcher wants to explore more machines with AI, they can do so; this part is not covered in the manuscript (Pany and Rao, 2004; Pany, 2023; Pany et al., 2025; Pany and Rao, 2002). The designed flexural mechanism opens an avenue for machine tool factories, specifically for linear movement feeding, if required. According to the results, the mechanisms can provide a cushioning effect to the drill, thereby preventing permanent rupture. Drilling quality remains the same, but the flexural mechanism absorbs the overload at the drill's weakest cross-section.

## 5 Conclusion

The research paper successfully develops a virtual NC machine tool within a PLM environment. The results of the virtual machine tool in the PLM platform indicate that this procedure can be applied to any machine, whether designed for general-purpose or specialized purposes. This successful implementation was achieved using SIEMENS NX 12 software. This interactive system generates results for both the user and the virtual environment. Designing

an m/c tool in the machine tool builder module of SIEMENS NX software creates a virtual environment that simulates a realistic manufacturing setup. The PLM platform identifies collision and gouge check detection, ensuring accuracy. The PLM platform allows the geometric model of the machine tool to which the kinematic chain is attached to be built. Attaching kinematic chains to all assembly components establishes a parent-child relationship among them. This hierarchical relationship, developed in the PLM platform, helps identify dependencies. As the number of axes increases, the system's complexity also increases. The next step is to assign junctions to all machine tool components. The last segment involves creating the virtual controller and the post-processor. The NCL file generated by the software is converted to "G and M" codes that the machine tool can easily accept. Every machine understands this file only. Irrespective of the machine, the controller decodes the movements into G-code and M-code. This code can be run on a machine with similar movements.

Furthermore, for the Flexural spindle head, drilled holes in the brass (specimen), the maximum diameter enlargement was 0.0448 mm (44.8  $\mu\text{m}$ ) at position "B28\_1". The "maximum average circularity" achieved was 26.4  $\mu\text{m}$  at positions B25\_1 and two others. Similarly, for the holes drilled by CNC, the maximum diameter enlargement was 104.3  $\mu\text{m}$  at position "B14\_1," and the maximum average circularity was 28.6  $\mu\text{m}$  at positions "B8\_1 and 2". The differences in diameter enlargement and maximum average circularity between the two methods were 59.5  $\mu\text{m}$  and 2.2  $\mu\text{m}$ , respectively. The initial cost of developing the flexural mechanism is very high. Further, the manufacturing process for building the assembly is also very high. Only specific linear motion and microdisplacement are provided by the flexural mechanisms. The mechanism does not provide a high displacement of more than 3 mm.

## Data availability statement

The original contributions presented in the study are included in the article/[Supplementary Material](#), further inquiries can be directed to the corresponding author.

## Author contributions

SSa: Conceptualization, Data curation, Formal Analysis, Funding acquisition, Investigation, Methodology, Project administration, Resources, Software, Supervision, Validation, Visualization, Writing – original draft, Writing – review and editing. SMS: Conceptualization, Data curation, Formal Analysis, Funding acquisition, Investigation, Methodology, Project administration, Resources, Software, Supervision, Validation, Visualization, Writing – original draft, Writing – review and editing. SSo: Conceptualization, Data curation, Formal Analysis, Funding acquisition, Investigation, Methodology, Project administration, Resources, Software, Supervision, Validation, Visualization, Writing – original draft, Writing – review and editing. MD: Conceptualization, Data curation, Formal Analysis, Funding acquisition, Investigation, Methodology, Project administration, Resources, Software, Supervision, Validation,

Visualization, Writing – original draft, Writing – review and editing. KB: Conceptualization, Data curation, Formal Analysis, Funding acquisition, Investigation, Methodology, Project administration, Resources, Software, Supervision, Validation, Visualization, Writing – original draft, Writing – review and editing. RC: Conceptualization, Data curation, Formal Analysis, Funding acquisition, Investigation, Methodology, Project administration, Resources, Software, Supervision, Validation, Visualization, Writing – original draft, Writing – review and editing. EN: Conceptualization, Data curation, Formal Analysis, Funding acquisition, Investigation, Methodology, Project administration, Resources, Software, Supervision, Validation, Visualization, Writing – original draft, Writing – review and editing.

## Funding

The author(s) declared that financial support was received for this work and/or its publication. The authors express their appreciation to King Saud University for funding this research through the Ongoing Research Funding program (ORF-2025-164). This article was co-funded by the European Union under the REFRESH–Research Excellence for Region Sustainability and High-tech Industries project number CZ.10.03.01/00/22\_003/0000048 *via* the Operational Programme Just Transition and has been done in connection with project Students Grant Competition SP2024/087 Specific Research of Sustainable Manufacturing Technologies "financed by the Ministry of Education, Youth and Sports and Faculty of Mechanical Engineering VŠB-TUO. The article has been done in connection with the project Students Grant Competition SP2024/087", Specific Research of Sustainable Manufacturing Technologies "financed by the Ministry of Education, Youth and Sports and Faculty of Mechanical Engineering VŠB-TUO".

## Conflict of interest

The author(s) declared that this work was conducted in the absence of any commercial or financial relationships that could be construed as a potential conflict of interest.

## Generative AI statement

The author(s) declared that generative AI was not used in the creation of this manuscript.

Any alternative text (alt text) provided alongside figures in this article has been generated by Frontiers with the support of artificial intelligence and reasonable efforts have been made to ensure accuracy, including review by the authors wherever possible. If you identify any issues, please contact us.

## Publisher's note

All claims expressed in this article are solely those of the authors and do not necessarily represent those of their

affiliated organizations, or those of the publisher, the editors and the reviewers. Any product that may be evaluated in this article, or claim that may be made by its manufacturer, is not guaranteed or endorsed by the publisher.

## References

Altintas, Y., Brecher, C., Week, M., and Witt, S. (2005). *Virtual machine tool*. 54 (2). 115–138. doi:10.1016/s0007-8506(07)60022-5

Bhole, K. S., and Janbandhu, M. (2018). “Design and development of double spiral shaped flexural feed stage for micro-drilling workstation,” in *International conference on advances in materials and manufacturing applications [IconAMMA 2017]* (Elsevier Ltd), 25468–25476.

Bhole, K., and Sonavane, V. (2018). “Parameter based method for three arm spiral shaped flexural bearing,” in *Materials today: proceedings* (Elsevier Ltd), 19380–19390.

Bhole, K., and Mastud, S. (2019). “Generalized design methodology for three-arm spiral cut compliant linear stage,” in *Operation management and systems engineering*. Editors A. Sachdeva, P. Kumar, O. P. Yadav, R. K. Garg, and A. Gupta (Springer Nature Singapore Pte Ltd), 127–144. doi:10.1007/978-981-15-6017-0\_8

Bohez, E. L. J. (2002). Five-axis milling machine tool kinematic chain design and analysis. *Int. J. Mach. Tools Manuf.* 42 (4), 505–520. doi:10.1016/S0890-6955(01)00134-1

Cao, X., and Li, B. (2022). “Design of micro five axis machien tool and research on virtual simulation machining,” in *3rd international conference on mechanical engineering and materials*. Bristol, England, United Kingdom: IOP Publishing Ltd, 1–14. doi:10.1088/1742-6596/2437/1/012071

Chan, D. S. K. (2003). Simulation modelling in virtual manufacturing analysis for integrated product and process design. *Assem. Autom.* 23 (1), 69–74. doi:10.1108/01445150310460114

Choi, S., Jung, K., and Do Noh, S. (2015). Virtual reality applications in manufacturing industries: past research, present findings, and future directions. *Concurr. Eng. Res. Appl.* 23 (1), 40–63. doi:10.1177/1063293X14568814

Ercetin, A., Der, O., Akkoyun, F., Gowdru Chandrashekappa, M., Şener, R., Çalışan, M., et al. (2024). Review of image processing methods for surface and tool condition assessments in machining. *J. Manuf. Mater. Process.* 8 (6), 244. doi:10.3390/jmmp8060244

Fischer, X., and Coutellier, D. (2006). “The interaction: a newway of designing,” in *Research in interactive design*. Editors X. Fischer and D. Coutellier 1st ed. (France: Springer), 1–15.

Gandhi, P., and Bhole, K. (2013). Characterization of ‘Bulk Lithography’ process for fabrication of three-dimensional microstructures. *J. Micro Nano-Manufacturing*. 1 (4), 1–8. doi:10.1115/1.4025461

Gandhi, P., Deshmukh, S., Ramtekkar, R., Bhole, K., and Baraki, A. (2013). On-axis’ linear focused spot scanning microstereolithography system: optomechatronic design, analysis and development. *J. Adv. Manuf. Syst.* 12 (1), 43–68. doi:10.1142/S0219686713500030

Kadir, A. A., Xu, X., and Hammerle, E. (2011). Virtual machine tools and virtual machining- A technological review. *Robot. Comput. Intergrated Manuf.* 27, 494–508. doi:10.1016/j.rcim.2010.10.003

Lagarrigue, P., Ramtekkar, R., and Bhole, K. (2006). *Virtual reality for NC machining improvement*. 1st ed. 2. France: Springer-Verlag. doi:10.1007/978-2-287-48370-7

Lee, R. S., and Lin, Y. H. (2010). Development of universal environment for constructing 5-axis virtual machine tool based on modified D-H notation and OpenGL. *Robot. Comput. Integrat. Manuf.* 26 (3), 253–262. doi:10.1016/j.rcim.2009.11.001

Lin, G. (2013). System and method for constructing virtual NC controllers for machine tool simulation.

Lin, R.-S., and Koren, Y. (2000). Ruled surface machining on five-axis CNC machine tools. *J. Manuf. Process.* 2 (1). doi:10.1016/S1526-6125(00)70010-7

Lisboa Borsatti, H., Ramos De Oliveira Santos Arthur, L., Miyashiro Rafael, E., Sugawara Juliana, K., Miyagi Eiji, P., and Junqueira, F. (2014). “3D virtual environments for manufacturing automation,” in *ABCm symposium series in mechatronics*, 559–567. Available online at: [www.revistapetrobras.com.br/revistapetrobras/files/pdfs/MateriadeCapa.pdf](http://www.revistapetrobras.com.br/revistapetrobras/files/pdfs/MateriadeCapa.pdf)

Pany, C. (2023). Large amplitude free vibrations analysis of prismatic and non-prismatic different tapered cantilever beams. *Pamukkale Univ. J. Eng. Sci.* 29 (4), 370–376. doi:10.5505/pajes.2022.02489

Pany, C., and Rao, G. V. (2002). Calculation of non-linear fundamental frequency of a cantilever beam using non-linear stiffness. *J. Sound. Vib.* 256 (4), 787–790. doi:10.1006/jsvi.2001.4224

Pany, C., and Rao, G. V. (2004). Large amplitude free vibrations of a uniform spring-hinged beam. *J. Sound. Vib.* 271 (3–5), 1163–1169. doi:10.1016/S0022-460X(03)00572-8

Pany, C., Desai, D., and de Rossi, W. (2025). Editorial: advances of finite element methods in the precision manufacturing processes. *Front. Manuf. Technol.* 5 (April), 2023–2025. doi:10.3389/fmtec.2025.1608699

Pimenvo, D. Y., da Silva, L. R., Ercetin, A., Der, O., Mikolajczyk, T., and Giasin, K. (2024). State-of-the art-review of application of image processing techniques for tool condition monitoring on conventional machining processes. *Int. J. Adv. Manuf. Technol.* 130, 57–85. doi:10.1007/s00170-023-12679-1

Puig, A., Perez-Vidal, L., and Tost, D. (2003). 3D simulation of tool machining. *Comput. Graph.* 27 (1), 99–106. doi:10.1016/S0097-8493(02)00248-0

Sanchez Gomez, C. A., Gil Castiblanco, L. E., and Arroyo Osorio, J. M. (2017). Building a virtual machine tool in a standard PLM platform. *Int. J. Interact. Des. Manuf.* 11 (2), 445–455. doi:10.1007/s12008-016-0312-9

Shinde, S. M., and Lekurwale, R. (2021). Design and development of three leg spiral curve flexural cartridge for micro drilling spindle head: a novel mechanism. *Int. J. Mechatronics Manuf. Syst.* 14 (1), 55–82. doi:10.1504/IJMMS.2021.115463

Shinde, S. M., and Lekurwale, R. R. (2018). Parametric mathematical modelling and aspect ratio optimization of eccentric spiral profile flexural bearing through finite element analysis studies. *SSRN Electron. J.* doi:10.2139/ssrn.3101366

Shinde, S., and Lekurwale, R. (2019). Behavioural study of spiral flexure disc by design of experiments and contour plots. *Ind. Eng. J.* 12 (8), 1–9. doi:10.26488/iej.12.8.1184

Shinde, S. M., and Lekurwale, R. R. (2022). Radial stiffness computation of single archimedes spiral plane supporting spring loaded in flexural mechanism mounted in spindle head of micro drilling machine tool. *Mech. Based Des. Struct. Mach.* 1 (5), 1–21. doi:10.1080/15397734.2022.2040363

Shinde, S., Lekurwale, R. R., Bhole, K. S., Oza, A. D., Patil, A. S., and Ramesh, R. (2022). 5-axis virtual machine tool centre building in PLM environment. *Int. J. Interact. Des. Manuf.* doi:10.1007/s12008-022-00974-2

Shinde, S. M., Bhole, K., and Diwan, M. (2023). Geometrical operating parameter’s analysis used in flexural cartridges. *Int. J. Interact. Des. Manuf.* 18, 7127–7157. doi:10.1007/s12008-023-01331-7

Siemens Product Lifecycle Management Software. (2013).NX 9 help documentation. Siemens.

Wang, D., and Yu, T. (2006). “Study on virtual intelligent assembly system for machine tool based on Multi-agent and petri - Net,” in *Proceedings of the fifth international conference on machine learning and cybernetics* (IEEE), 28–33.

Wang, Y., Wand, D., Zhang, S., Tang, Z., Wang, L., and Liu, Y. (2022). Design and development of five-axis machine tool with high accuracy, stiffness and efficiency for aero-engines casing manufacturing. *Chin. J. Aeronaut.* 35 (4), 485–496. doi:10.1016/j.cja.2021.04.001

Wang, Y., Ji, L., Dong, J., Liu, M., and Liu, J. (2023). Research on continuous machining strategy for five-axis machine tool: five-axis linkage to four-axis linkage. *Appl. Sci.* 13 (12), 7038. doi:10.3390/app13127038

Yuksel, E., Özlu, E., Oral, A., Tosun, F., İğrek, O. F., and Budak, E. (2020). “Design and analysis of a 5-Axis gantry CNC machine tool,” in *MATEC web of conferences*. doi:10.1051/matecconf/202031801019

## Supplementary material

The Supplementary Material for this article can be found online at: <https://www.frontiersin.org/articles/10.3389/fmech.2025.1609543/full#supplementary-material>